

Collision rates for ρ , ω and ϕ mesons at nonzero temperature

Kevin Haglin*

*National Superconducting Cyclotron Laboratory, Michigan State University
East Lansing, Michigan 48824-1321, USA*

(April 5, 2017)

Abstract

The ω and ϕ mesons are exceptionally narrow in vacua being about 8 and 4 MeV. At finite temperature they will scatter with other hadrons in their approach to equilibrium and thereafter. These dynamics induce broadening to the already unstable vector mesons which is calculated in the framework of relativistic kinetic theory. A rather complete set of low-lying mesons provide reaction partners whose interactions are modeled using effective Lagrangians. Collision rates for ρ and ω are found to be ~ 100 MeV at $T=200$ MeV while the rate for ϕ is ~ 25 MeV. Corresponding mean free paths are about 1 and 4 fm! Possible observable consequences are discussed.

PACS numbers: 25.75.+r, 14.40.Cs, 13.75.Lb

I. INTRODUCTION

Vector meson behaviour at nonzero temperature is particularly important for systems created in ultra-relativistic heavy-ion collisions. Details of their creation, propagation and decay greatly affect the overall many-body dynamics of the collisions and consequently the observed particle spectra. Pion or kaon correlations, strangeness production and absolute normalization of dilepton spectra are just a few features deeply linked to the way in which vector mesons behave in hot, strongly interacting matter. Primary emphases in past studies on this topic have been on possible mass shifts, modified dispersion relations and modifications to the widths [1–7]. Results for isoscalars and certain neutral isovectors have direct experimental significance since at minimum they might be observed through their decays into lepton pairs.

The ρ^0 meson decays strongly into oppositely charged pion pairs with a lifetime in the vacuum of ~ 1.3 fm/ c . The ω decays less often with a vacuum lifetime ~ 23 fm/ c and mostly into the pion triplet $\pi^+\pi^-\pi^0$ owing to its negative G-parity. Some difficulties would surely arise distinguishing one from the other in dilepton channels since they are nearly degenerate in mass—unless some spectacular differences in medium arose. The ϕ , on the other hand, is well removed with a vacuum mass above 1 GeV. It decays primarily into kaon pairs and $\pi\rho$ combinations with average lifetime ~ 44 fm/ c in the vacuum. At temperatures of the pion mass or above, broadening to a “full” width occurs in each of these mesons due to scattering since densities are nearly 1 hadron/fm³. Even rather nonreactive hadrons like the ϕ meson will scatter. Are the mean free paths for these particles about 1 fm or perhaps something much greater? Should any of them be expected to pass completely through reaction zones without interacting at all? The transverse size of the zone varies as $R = 1.2$ fm $\times A_p^{1/3}$ where A_p is the projectile mass number. For the heaviest beams expected in future experiments R is about 10 fm. Different outcomes could be expected depending on whether the average collision distances for the vector mesons are larger, nearly the same, or smaller than R .

In heavy-ion collisions at high energies the nuclei pass completely through each other and there is for a short time left behind a highly excited, very hot system of matter. Here is where one might expect to have quarks and gluons (partons) relatively free from nonperturbative effects. The partons are able to traverse distances larger than typical hadron sizes and one speaks of the quark-gluon plasma (QGP). Tremendous progress has been made recently in understanding some of the possible details of the QGP. A few specifics include thermalization time scales [9], chemical equilibration [10], particle production [11], temperature scenarios [12], and the role of minijets [13]. The system will eventually crossover from the plasma phase into a purely interacting hadronic state. Popular guesses as to where this occurs in temperature are near 200 MeV. Then for several fm/ c the system will interact strongly, cooling and expanding as it goes. Time and distance scales of interaction for the lightest hadrons are 1 to perhaps a few fm [14]. It cools and the pressure drops, expansion takes over and collisions cease to occur sometime about 30 or more fm/ c later, depending on such details as the roles of expansion and nucleation and subsequent degree of supercooling [15]. At this point the constituent hadrons (mostly pions) free stream. Understanding of the high temperature domain for the hadron phase has also improved through recent studies. Finite temperature behaviour of pions, ρ , ω , ϕ and a_1 mesons has been considered [5,7,16]. Temperature’s effect has been investigated using finite-temperature field theory at the one-

loop level for these mesons. But one of the basic sources of possible modification from vacuum properties occurs at the two-loop level and has been largely ignored—that of pure collisional modification. With regard to the ϕ meson Ko and Seibert [8] recently reported finding the full width including scattering was less than 10 MeV for all temperatures. But they neglected some important contributions which are included here and furthermore, their results were somewhat sensitive to the “in-medium” width of propagating kaons which was fixed first at 20 MeV and then 30 MeV for comparison. Improvements to this aspect of the calculation are made here by introducing a temperature and energy dependence to the widths of the exchanged particles.

This paper contains results of collisional effects on ρ , ω and ϕ mesons and is organized as follows. In the next section a model for the interacting hadronic system is discussed and its constituent degrees of freedom enumerated. Interactions are modeled with standard, yet simple Lagrangians consistent with a more elaborate and complete effective chiral Lagrangian. Coupling constants are chosen to give consistency with observed decays. Strong-interaction form factors are presented and briefly discussed. For some kinematic configurations in scattering the exchanged particles in t -channel graphs can become timelike and even approach mass shell. Pions and kaons are affected in this study and consequently acquire imaginary parts in their propagators which are estimated by computing temperature and momentum dependent collision rates. For simplicity, Breit-Wigner cross sections are used to account for interaction with pions, kaons and ρ mesons in these estimates. Section III contains the kinetic theoretic results for time and distance scales of interaction. Collision rates for all three vector mesons are computed first and then approximate mean free paths are obtained. Results are shown as a function of temperature in the range $100 \leq T \leq 200$ MeV. A short discussion and summary follows in Sec. IV highlighting possible consequences for ρ , ω and ϕ -related observables.

II. MODELING THE HADRONIC FIELDS

One might model the hadronic cooling stage as a thermal ensemble of low-lying hadrons: pions, kaons, ρ and $K^*(892)$ mesons as well as some heavier axial-vectors $a_1(1260)$, $b_1(1235)$ and $K_1(1270)$. The ϕ meson resides here also and like the others will be assumed to be thermalized. A posteriori this should be checked against average collision distances for validity. These particles are quantified as fields which interact according to the following Lagrangians [17,18]

$$\begin{aligned}
L_{VPP} &= g_{VPP} V^\mu P \overleftrightarrow{\partial}_\mu P \\
L_{VVP} &= g_{VVP} \epsilon_{\mu\nu\alpha\beta} \partial^\mu V^\nu \partial^\alpha V^\beta P \\
L_{AVP} &= g_{AVP} A_{\mu\nu} V^{\mu\nu} P,
\end{aligned}
\tag{2.1}$$

where the field strength tensors are $A_{\mu\nu} = \partial_\mu A_\nu - \partial_\nu A_\mu$ and similarly for $V^{\mu\nu}$. In the above expressions A , P and V refer to axial-vector, pseudoscalar and vector meson fields. Elementary processes can now be considered. To be completely general at this stage, consider the two diagrams shown in Fig. 1, where the species V will be a ρ , ω or a ϕ and the set $\{a, 1, 2, R, E\}$ are as-of-yet unspecified. Since hadronic cross sections tend to be dominated

by resonances, one naturally looks to $\rho\pi$ scattering through $a_1(1260)$, ρK scattering through $K_1(1270)$, $\omega\pi$ scattering through $b_1(1235)$ and to strange-particle possibilities for the ϕ . Although it can form $K_1(1770)$ and $K_4(2045)$ when scattering with kaons and K^* s, the branching ratios are very small leaving them inconsequential. There are also resonance possibilities in the non-strange sector. Scattering with pions is probable while forming $b_1(1235)$ or even $\rho(1450)$ mesons. The branching ratios are not firmly established, but tentative upper limits of 1.5 and 1 percent have been quoted [19]. Then in the t channel there are several seemingly equally important possible configurations since all three vector mesons can scatter with pions, kaons and a host of others. In considering diagrams for the general reaction with any of the vector mesons two problematic components immediately arise, namely, propagators and form factors.

Phase space allows the squared four-momentum of the exchanged particle to access timelike values and even become equal to its mass squared for those processes in which $m_1 + m_E < m_V$. If t is identically equal to m_E^2 then one has a true on-shell decay instead of scattering. This must be interpreted carefully so as to avoid double counting. The finite-temperature propagator at tree-level for the exchanged particles should, in principle, have the regular term $1/(p^2 - m^2)$ plus a term which goes like $2\pi\delta(p^2 - m^2)n_\beta$ [20]. If the second term is ignored while at the same time an imaginary part is introduced into the denominator of the first one by hand in order to account for the effect of the matter, i.e. $1/(p^2 - m^2 - im\Gamma)$, the result consistently accounts for scattering although somewhat phenomenologically. This is not meant to be a substitute for an evaluation of the two-loop diagrams which would consistently account for scattering plus higher-order corrections to decays at finite temperature, but instead an estimate of it. The appeal of the kinetic theory approach is that it is very straightforward and yet roughly captures the effect of the hot matter.

Hadrons necessitate the use of form factors since they are composite objects and have finite extent which can be seen when probed with higher and higher momentum transfers. A suppression of this region is physically imperative. The standard way to accomplish this is to insert a monopole form factor

$$F_\alpha(t) = \frac{\Lambda^2 - m_\alpha^2}{\Lambda^2 - t} \quad (2.2)$$

at each vertex in a t -channel diagram where α indicates a species for the exchanged particle. Besides the $\rho\pi\pi$ vertices in the reaction $\rho + \pi \rightarrow \rho + \pi$ which requires special attention to be discussed in a moment, Eq. (2.2) is adopted and a value of $\Lambda = 1.8$ GeV is taken for all vertices. Some uncertainty is duly noted since this parameter should really be species-dependent but in the absence of data with which one might compare this prescription is at least a reasonable approximation of the common finite-size features. The monopole form is normalized so that when the intermediate particle is on shell the form factor goes to 1. For most processes in meson-meson scattering this normalization is respected and $F > 1$ regions are kinematically inaccessible. However, the intermediate pion in the t channel of the reaction $\rho + \pi \rightarrow \rho + \pi$ is able to access this ‘‘hyper-normalized’’ region. To generalize the monopole form factor in a manner which is properly normalized when applied to the present case it is taken to be

$$\tilde{F}_\pi(t) = \frac{\Lambda^2 - t_{\max}}{\Lambda^2 - t} \quad (2.3)$$

where the maximum momentum transfer is

$$t_{\max} = m_\rho^2 + m_\pi^2 - \frac{1}{2s} \left((s + m_\rho^2 - m_\pi^2)(s + m_\pi^2 - m_\rho^2) - \lambda(s, m_\rho^2, m_\pi^2) \right). \quad (2.4)$$

The kinematical “triangle function” is $\lambda(x, y, z) = x^2 - 2x(y + z) + (y - z)^2$ [21] and a value $\Lambda = m_\rho$ is taken to soften the vertices.

Coupling constants naturally appear in the scattering amplitudes. They are adjusted in order to obtain the observed partial decay rates. Relevant rates for general decays are computed starting from the interactions in Eq. (2.1) to be

$$\begin{aligned} \Gamma_{V \rightarrow PP'} &= \frac{g_{VPP'}^2}{6\pi} \left(\frac{|\mathbf{p}|^3}{m_V^2} \right), \\ \Gamma_{V \rightarrow PV'} &= \frac{g_{VPV'}^2}{12\pi} |\mathbf{p}|^3, \\ \Gamma_{A \rightarrow VP} &= \frac{g_{AVP}^2}{6\pi} |\mathbf{p}| \left(\frac{(m_A^2 + m_V^2 - m_P^2)^2}{2m_A^2} + m_V^2 \right), \end{aligned} \quad (2.5)$$

where \mathbf{p} is the center-of-mass momentum of the decay products. From here one can get all the necessary coupling constants. They are listed in Table I. Notice that as they are used in the Lagrangians of Eq. (2.1), some are dimensionless and some carry units of inverse mass.

As mentioned already, timelike and intermediately propagating pions or kaons acquire imaginary parts due to the presence of the matter which are approximated by computing the dominant scattering rates. For instance, pions will scatter with other pions—a process dominated by the ρ resonance. They will also scatter with kaons to form $K^*(892)$ resonances. The rate at which each of these happens is roughly the density times the cross section times the relative velocity. More precisely, the contribution to the collision rate of particle b from pions is

$$\Gamma_b^{\text{coll}}(E, T) = \int ds \frac{d^3 p_\pi}{(2\pi)^3} f_\pi \sigma_{b\pi}(s) v_{\text{rel}} \delta \left(s - (p_b + p_\pi)^2 \right), \quad (2.6)$$

where f is the Bose-Einstein distribution function and

$$v_{\text{rel}} = \frac{\sqrt{(p_b \cdot p_\pi)^2 - 4m_b^2 m_\pi^2}}{E_b E_\pi}. \quad (2.7)$$

A Breit-Wigner form for the cross section

$$\sigma_{b\pi}(\sqrt{s}) = (2J_{\text{res}} + 1) \frac{\pi}{\mathbf{k}^2} \frac{\Gamma_{\text{res} \rightarrow b\pi}^2}{(\sqrt{s} - m_{\text{res}})^2 + \Gamma_{\text{res}}^2/4} \quad (2.8)$$

is used with \mathbf{k} being the center-of-mass momentum, “res” refers to the resonance through which it proceeds and b refers generally to pions or kaons. In the case of kaons, resonances K^* and $K_1(1270)$ are allowed since scattering with pions and with ρ mesons are frequent. The width is a function of the three-momentum separately and is therefore frame-dependent but determined by the hadron gas. Results for pions and kaons are presented in Figs. 2a and b respectively, each for temperatures 100, 150 and 200 MeV. Depending on the temperature

and on the pion or kaon momenta, widths vary from 20 to 200 MeV. Results similar to these were recently obtained for the momentum dependent scattering rate of ω mesons at finite temperature using this prescription [22]. These broad widths could drastically modify the propagators and consequently modify the vector-meson reactions. Propagators for intermediate pions and kaons, indicated generally by species b , will henceforth be

$$i\Delta_b(p^2, E, T) = \frac{i}{p^2 - m_b^2 - im_b\Gamma_b(E, T)}. \quad (2.9)$$

III. TIME AND DISTANCE SCALES OF INTERACTION

The hot matter created in heavy-ion collisions of the type considered here is populated mostly by pions and kaons and one knows their collision times are ~ 1 fm/ c at high temperatures [23–25]. The system is temporarily supported by its own collisions. Thermodynamic estimates of pion and kaon abundances are 0.3 and 0.1 per fm³ for high temperatures while they are 0.15, 4.7×10^{-2} and 1.9×10^{-2} per fm³ for ρ , ω and ϕ mesons at $T = 200$ MeV. It is interesting to see just how often they will collide in this model for the reaction zone in the moments before freezeout.

A. Collision Rates

For a general (bosonic) reaction involving the vector V and having the form $V+a \rightarrow 1+2$, the kinetic theory expression for an average scattering rate is

$$\begin{aligned} \bar{\Gamma}_V^{\text{coll}} = & \frac{1}{n_V} d_V d_a \int d^3\bar{p}_V d^3\bar{p}_a d^3\bar{p}_1 d^3\bar{p}_2 |\bar{\mathcal{M}}|^2 (2\pi)^4 \delta^4(p_V + p_a - p_1 - p_2) \\ & \times f_V f_a (1 + f_1) (1 + f_2) \end{aligned} \quad (3.1)$$

where $d^3\bar{p}_V = d^3p_V/2E_V(2\pi)^3$ and similarly for the others, where the bar over the squared scattering amplitude indicates that an initial spin average and final spin sum must be done, where f is again the Bose-Einstein distribution, the d s are degeneracy factors, and the number density of V s is

$$n_V = d_V \int \frac{d^3p_V}{(2\pi)^3} f_V. \quad (3.2)$$

Reduction of phase space is accomplished with the aid of the four-momentum conserving delta function and the remaining integration is done numerically. Processes considered in this study are enumerated in Table II in no particular order and their scattering amplitudes are relegated to the appendix.

i. ρ meson

Elastic $\rho + \pi$ scattering proceeds through s and t channels where π, ω, ϕ, a_1 , and $\omega(1390)$ might be intermediate or exchanged. There are ten Feynman graphs in total. Elastic scattering with kaons may proceed through both s and t channels (two Feynman graphs) with

$K_1(1270)$ as the exchanged particle. Though interference effects are found to be quite modest the first ten graphs must be added coherently upon squaring, i.e. $|\mathcal{M}_1 + \mathcal{M}_2 + \dots + \mathcal{M}_{10}|^2$. The result is then added to the coherent sum of the two kaon graphs $|\mathcal{M}_{11} + \mathcal{M}_{12}|^2$. In addition to these 12 graphs there is some possibility of $\rho+\rho$ scattering. It has been estimated to be relatively unimportant, e.g. something like 5 MeV at 200 MeV temperature so it will not be discussed further. At the highest temperature considered the scattering rate from the kaon contribution is 66 MeV while the sum of pion and kaon contributions is 115.5 MeV. Results are shown separately and then summed in Fig. 3. As expected, the pions account for most of the scattering throughout the entire temperature domain but at higher temperatures the kaon contribution becomes nearly 50% of the pions'. At highest temperature the collision rate is something like 75% of the vacuum decay rate.

ii. ω meson

The dominant contribution for ω scattering is from pions as well, this time intermediate ρ and $b_1(1235)$ mesons are important. Four graphs are needed to account for both s and t channels and must be added coherently upon squaring $|\mathcal{M}_1 + \mathcal{M}_2 + \dots + \mathcal{M}_4|^2$. Strange-particle processes involving the ω are suppressed as compared with the ρ since there is no resonance playing a role as prominent as K_1 . But in their place a sizable contribution comes from $\omega + \pi \rightarrow \pi + \pi$. Two diagrams must be computed whose scattering amplitudes are listed along with all the others in the appendix. Resulting contributions are shown in Fig. 4. A fairly large rate is obtained at high temperature. The unstable ω , whose vacuum width is about 8 MeV, will have an “effective width” of 103 MeV assuming its decays are not drastically altered. Recent suggestions were made that a signature of dense hadronic matter might be enhanced e^+e^- production with invariant mass very near m_ω due to three pion initial states $\pi^+\pi^-\pi^0$ and owing to the high densities [26]. A broadening to the ω of such an extent as 95 MeV might significantly affect the possible signature.

iii. ϕ meson

No single channel dominates the ϕ like the other vector mesons considered here since there is no strong $\phi + x$ resonance where x might be a pion, kaon, K^* , or others. Many channels must therefore be considered and are listed in table II. For illustration purposes the channel $\phi + \rho \rightarrow K_1(1270) + K$ is isolated and shown in Fig. 5. The solid curve results from using an energy and temperature dependent width in the propagator for the exchanged kaon. Notably, the rate is about 3 MeV at high temperatures. To visualize the sensitivity of the energy dependence of Γ_K , results are also shown wherein fixed widths of 20 and 30 MeV are used instead of Eq. (2.6). Clearly these energy dependences are quite important, especially for the highest temperatures. This channel is not an obvious candidate for a large contribution to the rate yet turns out to be important. As expected from simple number-density arguments, a large contribution comes from the reaction $\phi + \pi \rightarrow K^* + K$. Others are important as can be seen from Fig. 6 which compares contributions from a subset of the processes listed in Table II. The overall normalization of the $\phi + \rho \rightarrow K_1(1270) + K$ reaction is somewhat of a surprise. Other small surprises are the strengths of $\phi + \pi \rightarrow \pi + \omega$ (long-dashed curve), $\phi + K^* \rightarrow \pi + K$ (lower-dotted curve) and $\phi + K \rightarrow \pi + K^*$ (quadruple-dot-dashed curve). At high temperatures several channels contribute nearly equally strongly as can be

seen from the column of $T = 200$ MeV results shown numerically in Table II. Although quite small, contribution from the $\rho(1450)$ channel (triple-dot-dashed curve) is also shown in the figure.

Then, the sum of all contributions is shown in Fig. 7. At 100 MeV temperature the rate is only 2.4 MeV. Modification of the ϕ width due to the matter is modest. But as the temperature rises to 150 MeV the scattering rate is 8.6 MeV and at $T = 200$ MeV, the rate goes to 27.4 MeV. Modification of this extent for a particle whose vacuum decay width is of order 4 MeV is quite significant.

B. Mean Free Paths

The “rule of thumb” for hadronic collision distances in finite temperature media are of order 1 fm. For ρ and possibly ω mesons this is reasonable since they react vigorously with pions. However, standard lore has it that only a small fraction of ϕ mesons in these media will decay or interact before leaving. To test this idea for how frequently they interact, their mean free paths must be computed. They can be approximated by

$$\bar{\lambda}_V = \bar{v}_V / \bar{\Gamma}_V^{\text{coll}} . \quad (3.3)$$

Collision rates are already obtained, what remains to compute are average velocities. They are estimated with

$$\bar{v}_V = \frac{d_V}{n_V} \int \frac{d^3 p_V}{(2\pi)^3} f_V \frac{|\mathbf{p}_V|}{E_V} \quad (3.4)$$

to be monotonically increasing functions of temperature. Values for the ϕ of $\bar{v}_\phi = 0.46, 0.54$ and $0.61 \times c$ are obtained at temperatures 100, 150 and 200 MeV, respectively. This translates into mean free paths for the ϕ of 38.2, 14.9 and 4.4 fm at the corresponding temperatures. Results for ρ, ω and ϕ and for arbitrary temperatures $100 \leq T \leq 200$ MeV are shown in Fig 8. The higher-temperature results for the ϕ are not consistent with common lore and are therefore worth restating in more direct terms. The mean free path $\bar{\lambda}_\phi$ is shorter than a typical transverse size for colliding nuclei which means on average, the ϕ will indeed scatter before leaving the reaction zone. Consequently, the assumption made earlier about its momentum distribution being thermal is probably not unreasonable.

IV. SUMMARY

In this paper results were reported for collision rates of ρ, ω and ϕ mesons at nonzero temperature. Special attention was given to modification of the zero-temperature scalar-boson propagator due to the presence of matter since it is involved quite crucially in certain reactions. The real part of this modification was ignored while the imaginary part was computed using a simple expression from kinetic theory and then inserted by hand.

At low temperatures, by which 100 MeV or so is meant, the collision rates for all three were quite small $\sim 10, 6,$ and 2 MeV for ρ, ω and ϕ . Results for each of them rises monotonically as the number densities of pions and kaons increase. As temperatures rise

above the pion mass, the number densities of species other than pions and kaons become large enough so that collisions with the ϕ are more frequent. Scattering of ϕ mesons with ρ and K^* mesons becomes significant around 150 MeV temperature while at high temperatures several processes contribute nearly equally resulting in a total rate of 27.2 MeV at $T = 200$ MeV. At this extreme, the mean free path of ϕ mesons is 4.4 fm! One could be justified in using thermal distributions for this species [27]. These time and distance scales could have noticeable consequences on some observables at least for ω and ϕ -related ones. A place to look for modification might be in dilepton invariant mass spectra. For instance, the ϕ peak might appear rather differently and may not be so clearly visible above the tail of $\pi^+\pi^-$ annihilations. This broadening or “melting” of the resonances could have an affect on the overall normalization of low-mass e^+e^- production since it depends on a sum over all scattering energies for the hadrons (pions). The broad widths will change the normalization by roughly $(\Gamma_{\text{narrow}}/\Gamma_{\text{broad}})^2$. In the cases of ρ and ω at highest temperature these factors are 1/3 and 1/150!

A final remark is perhaps in order about the limitations of this approach to studying collisional phenomena as compared with that of purely field theory. In field theory at finite temperature the vector meson self-energy approximated with one-loop diagrams gives rise to on-shell decays within matter. This is so because there is a basic connection between the statistical mechanical collision rate Γ and the imaginary part of the field-theoretic finite-temperature self-energy Π [28]. The two-loop contribution to Π acquires an imaginary part at $T \neq 0$ due to scattering plus higher-order vertex corrections and phase-space broadening of the final states in the above mentioned decays. Mass modification due to the matter is also present in such calculations since the real parts are included. Kinetic theory calculations, on the other hand, like the one presented here simply cannot do all this. Computing the self-energy to two-loop order at finite-temperature requires much more effort than invested in this work but should be done for a consistency check.

ACKNOWLEDGEMENTS

It is a pleasure to thank S. Pratt for valuable discussions. This work was supported by the National Science Foundation under grant number PHY-9403666.

APPENDIX: AMPLITUDES

Scattering amplitudes are included here for completeness. The processes to which they apply are enumerated in Table II of the text. Many of them contain the form factor $F(t)$ which is Eq. (2.2) in the text and the first two ρ -meson amplitudes contain the form factor $\tilde{F}_\pi(t)$ of Eq. (2.3). Every external spin-one particle in a Feynman graph introduces a polarization four-vector ϵ^μ . It depends on some momentum \mathbf{p} as well as a spin index λ . In the amplitudes written here, the spin indices are all suppressed. Upon squaring these amplitudes spin sums must be performed, giving

$$\sum_{\lambda} \epsilon_{\mu}^{(\lambda)}(\mathbf{p}) \epsilon_{\nu}^{(\lambda)*}(\mathbf{p}) = - \left(g_{\mu\nu} - p_{\mu} p_{\nu} / m^2 \right). \quad (\text{A1})$$

i. ρ scattering amplitudes

The individual amplitudes are

$$\begin{aligned}
\mathcal{M}_1^{(\rho)} &= g_{\rho\pi\pi}^2 \epsilon^\mu(p_\rho) (2p_\pi + p_\rho)_\mu \epsilon^\nu(p_{\rho'}) (2p_{\rho'} + p_{\pi'})_\nu \Delta_\pi(s, E, T) \\
\mathcal{M}_2^{(\rho)} &= g_{\rho\pi\pi}^2 \tilde{F}_\pi^2(t) \epsilon^\mu(p_\rho) (2p_{\pi'} - p_\rho)_\mu \epsilon^\nu(p_{\rho'}) \\
&\quad \times (2p_\pi - p_{\rho'})_\nu \Delta_\pi(l^2, E, T) \\
\mathcal{M}_3^{(\rho)} &= g_{\rho\pi\omega}^2 \epsilon_{\mu\nu\alpha\beta} p_\rho^\mu \epsilon^\nu(p_\rho) q^\alpha \left(g^{\beta\tau} - q^\beta q^\tau / m_\omega^2 \right) q^\sigma \epsilon^\lambda(p_{\rho'}) \\
&\quad \times p_{\rho'}^\kappa \epsilon_{\kappa\lambda\sigma\tau} \frac{1}{s - m_\omega^2 - im_\omega \Gamma_\omega} \\
\mathcal{M}_4^{(\rho)} &= g_{\rho\pi\omega}^2 F_\omega^2(t) \epsilon_{\mu\nu\alpha\beta} p_\rho^\mu \epsilon^\nu(p_\rho) l^\alpha \left(g^{\beta\tau} - l^\beta l^\tau / m_\omega^2 \right) l^\sigma \epsilon^\lambda(p_{\rho'}) \\
&\quad \times p_{\rho'}^\kappa \epsilon_{\kappa\lambda\sigma\tau} \frac{1}{l^2 - m_\omega^2 - im_\omega \Gamma_\omega} \\
\mathcal{M}_5^{(\rho)} &= g_{\rho\pi\phi}^2 \epsilon_{\mu\nu\alpha\beta} p_\rho^\mu \epsilon^\nu(p_\rho) q^\alpha \left(q^{\beta\tau} - q^\beta q^\tau / m_\phi^2 \right) q^\sigma \epsilon^\lambda(p_{\rho'}) \\
&\quad \times p_{\rho'}^\kappa \epsilon_{\kappa\lambda\sigma\tau} \frac{1}{s - m_\phi^2 - im_\phi \Gamma_\phi} \\
\mathcal{M}_6^{(\rho)} &= g_{\rho\pi\phi}^2 F_\phi^2(t) \epsilon_{\mu\nu\alpha\beta} p_\rho^\mu \epsilon^\nu(p_\rho) l^\alpha \left(q^{\beta\tau} - l^\beta l^\tau / m_\phi^2 \right) l^\sigma \epsilon^\lambda(p_{\rho'}) \\
&\quad \times p_{\rho'}^\kappa \epsilon_{\kappa\lambda\sigma\tau} \frac{1}{l^2 - m_\phi^2 - im_\phi \Gamma_\phi} \\
\mathcal{M}_7^{(\rho)} &= g_{\rho a_1 \pi}^2 \epsilon_\sigma(p_\rho) \left[p_\rho^\mu g_{\nu\sigma} - p_\rho^\nu g_{\mu\sigma} \right] \left[q_\mu g_{\nu\sigma} - q_\nu g_{\mu\sigma} \right] \\
&\quad \times \left[g^{\alpha\beta} - q^\alpha q^\beta / m_{a_1}^2 \right] \left[q_\kappa g_{\lambda\beta} - q_\lambda g_{\kappa\beta} \right] \\
&\quad \times \left[p_{\rho'}^\kappa g^{\lambda\tau} - p_{\rho'}^\lambda g^{\kappa\tau} \right] \epsilon_\tau(p_{\rho'}) \frac{1}{s - m_{a_1}^2 - im_{a_1} \Gamma_{a_1}} \\
\mathcal{M}_8^{(\rho)} &= g_{\rho a_1 \pi}^2 F_{a_1}^2(t) \epsilon_\sigma(p_\rho) \left[p_\rho^\mu g_{\nu\sigma} - p_\rho^\nu g_{\mu\sigma} \right] \left[l_\mu g_{\nu\sigma} - l_\nu g_{\mu\sigma} \right] \\
&\quad \times \left[g^{\alpha\beta} - l^\alpha l^\beta / m_{a_1}^2 \right] \left[l_\kappa g_{\lambda\beta} - l_\lambda g_{\kappa\beta} \right] \\
&\quad \times \left[p_{\rho'}^\kappa g^{\lambda\tau} - p_{\rho'}^\lambda g^{\kappa\tau} \right] \epsilon_\tau(p_{\rho'}) \frac{1}{l^2 - m_{a_1}^2 - im_{a_1} \Gamma_{a_1}} \\
\mathcal{M}_9^{(\rho)} &= g_{\rho\pi\omega^*}^2 \epsilon_{\mu\nu\alpha\beta} p_\rho^\mu \epsilon^\nu(p_\rho) q^\alpha \left(g^{\beta\tau} - q^\beta q^\tau / m_{\omega^*}^2 \right) q^\sigma \epsilon^\lambda(p_{\rho'}) \\
&\quad \times p_{\rho'}^\kappa \epsilon_{\kappa\lambda\sigma\tau} \frac{1}{s - m_{\omega^*}^2 - im_{\omega^*} \Gamma_{\omega^*}} \\
\mathcal{M}_{10}^{(\rho)} &= g_{\rho\pi\omega^*}^2 F_{\omega^*}^2(t) \epsilon_{\mu\nu\alpha\beta} p_\rho^\mu \epsilon^\nu(p_\rho) l^\alpha \left(g^{\beta\tau} - l^\beta l^\tau / m_{\omega^*}^2 \right) l^\sigma \epsilon^\lambda(p_{\rho'}) \\
&\quad \times p_{\rho'}^\kappa \epsilon_{\kappa\lambda\sigma\tau} \frac{1}{l^2 - m_{\omega^*}^2 - im_{\omega^*} \Gamma_{\omega^*}} \\
\mathcal{M}_{11}^{(\rho)} &= g_{\rho K_1 K}^2 \epsilon_\sigma(p_\rho) \left[p_\rho^\mu g_{\nu\sigma} - p_\rho^\nu g_{\mu\sigma} \right] \left[q_\mu g_{\nu\sigma} - q_\nu g_{\mu\sigma} \right] \\
&\quad \times \left[g^{\alpha\beta} - q^\alpha q^\beta / m_{K_1}^2 \right] \left[q_\kappa g_{\lambda\beta} - q_\lambda g_{\kappa\beta} \right] \\
&\quad \times \left[p_{\rho'}^\kappa g^{\lambda\tau} - p_{\rho'}^\lambda g^{\kappa\tau} \right] \epsilon_\tau(p_{\rho'}) \frac{1}{s - m_{K_1}^2 - im_{K_1} \Gamma_{K_1}}
\end{aligned}$$

$$\begin{aligned}
\mathcal{M}_{12}^{(\rho)} &= g_{\rho K_1 K}^2 F_{K_1}^2(t) \epsilon_\sigma(p_\rho) \left[p_\rho^\mu g_{\nu\sigma} - p_\rho^\nu g_{\mu\sigma} \right] \left[\tilde{l}_\mu g_{\nu\sigma} - \tilde{l}_\nu g_{\mu\alpha} \right] \\
&\quad \times \left[g^{\alpha\beta} - \tilde{l}^\alpha \tilde{l}^\beta / m_{K_1}^2 \right] \left[\tilde{l}_\kappa g_{\lambda\beta} - \tilde{l}_\lambda g_{\kappa\beta} \right] \\
&\quad \times \left[p_{\rho'}^\kappa g^{\lambda\tau} - p_{\rho'}^\lambda g^{\kappa\tau} \right] \epsilon_\tau(p_{\rho'}) \frac{1}{\tilde{l}^2 - m_{K_1}^2 - im_{K_1} \Gamma_{K_1}}
\end{aligned} \tag{A2}$$

where the primed variables indicate final states, where ω^* is shorthand for $\omega(1390)$, $q = p_\rho + p_\pi$ and naturally $s = q^2$, $\tilde{q} = p_\rho + p_K$, $l = p_{\pi'} - p_\rho$ and $\tilde{l} = p_{K'} - p_\rho$, and where Eq. (2.9) has been utilized for compactness.

ii. ω scattering amplitudes

$$\begin{aligned}
\mathcal{M}_1^{(\omega)} &= g_{\rho b_1 \pi}^2 \epsilon_\sigma(p_\omega) \left[p_\omega^\mu g_{\nu\sigma} - p_\omega^\nu g_{\mu\sigma} \right] \left[q_\mu g_{\nu\sigma} - q_\nu g_{\mu\alpha} \right] \\
&\quad \times \left[g^{\alpha\beta} - q^\alpha q^\beta / m_{b_1}^2 \right] \left[q_\kappa g_{\lambda\beta} - q_\lambda g_{\kappa\beta} \right] \\
&\quad \times \left[p_{\omega'}^\kappa g^{\lambda\tau} - p_{\omega'}^\lambda g^{\kappa\tau} \right] \epsilon_\tau(p_{\omega'}) \frac{1}{s - m_{b_1}^2 - im_{b_1} \Gamma_{b_1}} \\
\mathcal{M}_2^{(\omega)} &= g_{\rho b_1 \pi}^2 F_{b_1}^2(t) \epsilon_\sigma(p_\omega) \left[p_\omega^\mu g_{\nu\sigma} - p_\omega^\nu g_{\mu\sigma} \right] \left[l_\mu g_{\nu\sigma} - l_\nu g_{\mu\alpha} \right] \\
&\quad \times \left[g^{\alpha\beta} - l^\alpha l^\beta / m_{a_1}^2 \right] \left[l_\kappa g_{\lambda\beta} - l_\lambda g_{\kappa\beta} \right] \\
&\quad \times \left[p_{\omega'}^\kappa g^{\lambda\tau} - p_{\omega'}^\lambda g^{\kappa\tau} \right] \epsilon_\tau(p_{\omega'}) \frac{1}{l^2 - m_{b_1}^2 - im_{b_1} \Gamma_{b_1}} \\
\mathcal{M}_3^{(\omega)} &= g_{\omega \pi \rho}^2 \epsilon_{\mu\nu\alpha\beta} p_\omega^\mu \epsilon^\nu(p_\omega) q^\alpha \left(g^{\beta\tau} - q^\beta q^\tau / m_\rho^2 \right) q^\sigma \epsilon^\lambda(p_{\omega'}) \\
&\quad \times p_{\omega'}^\kappa \epsilon_{\kappa\lambda\sigma\tau} \frac{1}{s - m_\rho^2 - im_\rho \Gamma_\rho} \\
\mathcal{M}_4^{(\omega)} &= g_{\omega \pi \rho}^2 F_\rho^2(t) \epsilon_{\mu\nu\alpha\beta} p_\omega^\mu \epsilon^\nu(p_\omega) l^\alpha \left(g^{\beta\tau} - l^\beta l^\tau / m_\rho^2 \right) l^\sigma \epsilon^\lambda(p_{\omega'}) \\
&\quad \times p_{\omega'}^\kappa \epsilon_{\kappa\lambda\sigma\tau} \frac{1}{l^2 - m_\rho^2 - im_\rho \Gamma_\rho} \\
\mathcal{M}_5^{(\omega)} &= g_{\omega \pi \rho} g_{\rho \pi \pi} \epsilon_{\mu\nu\alpha\beta} p_\omega^\mu \epsilon^\nu(p_\omega) q^\alpha \left(g^{\beta\lambda} - q^\beta q^\lambda / m_\rho^2 \right) (p_{\pi'} - p_{\pi''})_\lambda \\
&\quad \times \frac{1}{s - m_\rho^2 - im_\rho \Gamma_\rho} \\
\mathcal{M}_6^{(\omega)} &= g_{\omega \pi \rho} g_{\rho \pi \pi} F_\rho^2(t) \epsilon_{\mu\nu\alpha\beta} p_\omega^\mu \epsilon^\nu(p_\omega) l^\alpha \left(g^{\beta\lambda} - l^\beta l^\lambda / m_\rho^2 \right) \\
&\quad \times (p_\pi + p_{\pi'})_\lambda \frac{1}{l^2 - m_\rho^2 - im_\rho \Gamma_\rho}
\end{aligned} \tag{A3}$$

where this time $q = p_\omega + p_\pi$ and $l = p_{\pi'} - p_\omega$.

ii. ϕ scattering amplitudes

The scattering amplitudes for ϕ reactions are

$$\mathcal{M}_1^{(\phi)} = g_{\phi K K} g_{K_1 \rho K} F_K^2(t) \epsilon^\kappa(p_\phi) (2p_K - p_\phi)_\kappa \epsilon^\sigma(p_{K_1})$$

$$\begin{aligned}
& \times [p_{K_1\mu}g_{\sigma\nu} - p_{K_1\nu}g_{\sigma\mu}] [p_\rho^\mu g^{\lambda\nu} - p_\rho^\nu g^{\lambda\mu}] \epsilon_\lambda(p_\rho) \Delta_K(\tilde{l}^2, E, T) \\
\mathcal{M}_2^{(\phi)} &= g_{\phi KK} g_{K^*\pi K} F_K^2(t) \epsilon^\mu(p_\phi) (2p_K - p_\phi)_\mu \epsilon^\nu(p_{K^*}) (2p_\pi - p_{K^*})_\nu \\
& \quad \times \Delta_K(\tilde{l}^2, E, T) \\
\mathcal{M}_3^{(\phi)} &= g_{\phi KK} g_{K^*\pi K} F_K^2(t) \epsilon^\mu(p_\phi) (2p_K - p_\phi)_\mu \epsilon^\nu(p_{K^*}) (2p_\pi - p_{K^*})_\nu \\
& \quad \times \Delta_K(\tilde{l}^2, E, T) \\
\mathcal{M}_4^{(\phi)} &= g_{\phi KK} g_{K_1\rho K} F_K^2(t) \epsilon^\kappa(p_\phi) (2p_K - p_\phi)_\kappa \epsilon^\sigma(p_{K_1}) \\
& \quad \times [p_{K_1\mu}g_{\sigma\nu} - p_{K_1\nu}g_{\sigma\mu}] [p_\rho^\mu g^{\lambda\nu} - p_\rho^\nu g^{\lambda\mu}] \epsilon_\lambda(p_\rho) \Delta_K(\tilde{l}^2, E, T) \\
\mathcal{M}_5^{(\phi)} &= g_{\phi\rho\pi} g_{\rho\pi\pi} F_\pi^2(t) \epsilon_{\mu\nu\alpha\beta} p_\phi^\mu \epsilon^\nu(p_\phi) p_\rho^\alpha \epsilon^\beta(p_\rho) \epsilon^\lambda(p_\rho) (2p_\pi - p_\rho)_\lambda \Delta_\pi(l^2, E, T) \\
\mathcal{M}_6^{(\phi)} &= g_{\phi\rho\pi} g_{a_1\rho\pi} F_\pi^2(t) \epsilon_{\mu\nu\alpha\beta} p_\phi^\mu \epsilon^\nu(p_\phi) p_\rho^\alpha \epsilon^\beta(p_\rho) \epsilon^\sigma(p_{a_1}) \\
& \quad \times [p_{a_1\tau}g_{\sigma\kappa} - p_{a_1\kappa}g_{\sigma\tau}] [p_\rho^\tau g^{\lambda\kappa} - p_\rho^\kappa g^{\lambda\tau}] \epsilon_\lambda(p_\rho) \Delta_\pi(l^2, E, T) \\
\mathcal{M}_7^{(\phi)} &= g_{\phi b_1\pi} g_{\omega b_1\pi} \epsilon_\sigma(p_\phi) [p_\phi^\mu g_{\nu\sigma} - p_\phi^\nu g_{\mu\sigma}] [q_\mu g_{\nu\sigma} - q_\nu g_{\mu\alpha}] \\
& \quad \times [g^{\alpha\beta} - q^\alpha q^\beta / m_{a_1}^2] [q_\kappa g_{\lambda\beta} - q_\lambda g_{\kappa\beta}] \\
& \quad \times [p_\omega^\kappa g^{\lambda\tau} - p_\omega^\lambda g^{\kappa\tau}] \epsilon_\tau(p_\omega) \frac{1}{s - m_{b_1}^2 - im_{b_1}\Gamma_{b_1}} \\
\mathcal{M}_8^{(\phi)} &= g_{\phi b_1\pi} g_{\omega b_1\pi} F_{b_1}^2(t) \epsilon_\sigma(p_\phi) [p_\phi^\mu g_{\nu\sigma} - p_\phi^\nu g_{\mu\sigma}] [l_\mu g_{\nu\sigma} - l_\nu g_{\mu\alpha}] \\
& \quad \times [g^{\alpha\beta} - l^\alpha l^\beta / m_{b_1}^2] [l_\kappa g_{\lambda\beta} - l_\lambda g_{\kappa\beta}] \\
& \quad \times [p_\omega^\kappa g^{\lambda\tau} - p_\omega^\lambda g^{\kappa\tau}] \epsilon_\tau(p_\omega) \frac{1}{l^2 - m_{b_1}^2 - im_{b_1}\Gamma_{b_1}} \\
\mathcal{M}_9^{(\phi)} &= g_{\phi KK}^2 \epsilon^\mu(p_\phi) (2p_K + p_\phi)_\mu \epsilon^\nu(p_{\phi'}) (2p_{K'} + p_{\phi'})_\nu \\
& \quad \times \frac{1}{s - m_K^2 - im_K\Gamma_K(E, T)} \\
\mathcal{M}_{10}^{(\phi)} &= g_{\phi KK}^2 F_K^2(t) \epsilon^\mu(p_\phi) (2p_{K'} - p_\phi)_\mu \epsilon^\nu(p_{\phi'}) (2p_{K'} - p_{\phi'})_\nu \\
& \quad \times \Delta_K(\tilde{l}^2, E, T) \\
\mathcal{M}_{11}^{(\phi)} &= g_{\phi KK} g_{\rho KK} F_K^2(t) \epsilon^\mu(p_\phi) (2p_{K'} - p_\phi)_\mu \epsilon^\nu(p_\rho) (2p_K - p_\rho)_\nu \\
& \quad \times \Delta_K(\tilde{l}^2, E, T) \\
\mathcal{M}_{12}^{(\phi)} &= g_{\phi KK}^2 F_K^2(t) \epsilon^\mu(p_\phi) (2p_K - p_\phi)_\mu \epsilon^\nu(p_{\bar{\phi}}) (2p_{K'} - p_{\bar{\phi}})_\nu \\
& \quad \times \Delta_K(\tilde{l}^2, E, T) \\
\mathcal{M}_{13}^{(\phi)} &= g_{\phi\rho\pi} g_{K^*\pi K} F_\pi^2(t) \epsilon_{\mu\nu\alpha\beta} p_\phi^\mu \epsilon^\nu(p_\phi) p_\rho^\alpha \epsilon^\beta(p_\rho) \epsilon^\lambda(p_{K^*}) (2p_K - p_{K^*})_\lambda \\
& \quad \times \Delta_\pi(l^2, E, T) \\
\mathcal{M}_{14}^{(\phi)} &= g_{\phi\rho\pi} g_{K^*\pi K} F_\pi^2(t) \epsilon_{\mu\nu\alpha\beta} p_\phi^\mu \epsilon^\nu(p_\phi) p_\rho^\alpha \epsilon^\beta(p_\rho) \epsilon^\lambda(p_{K^*}) (2p_K - p_{K^*})_\lambda \\
& \quad \times \Delta_\pi(l^2, E, T) \\
\mathcal{M}_{15}^{(\phi)} &= g_{\phi KK} g_{\rho KK} F_\pi^2(t) \epsilon^\mu(p_\phi) (2p_{K'} - p_\phi)_\mu \epsilon^\nu(p_\rho) (2p_K - p_\rho)_\nu \Delta_K(\tilde{l}^2, E, T) \\
\mathcal{M}_{16}^{(\phi)} &= g_{\phi\rho^*\pi} g_{\rho^*\pi\pi} \epsilon_{\mu\nu\alpha\beta} p_\phi^\mu \epsilon^\nu(p_\phi) (p_\phi + p_\pi)^\alpha [g^{\beta\lambda} - (p_\phi + p_\pi)^\beta (p_\phi + p_\pi)^\lambda]
\end{aligned}$$

$$\begin{aligned}
& \times (p_{\pi'} - p_{\pi''})_\lambda \frac{1}{s - m_{\rho^*}^2 - im_{\rho^*}\Gamma_{\rho^*}} \\
\mathcal{M}_{17}^{(\phi)} = & g_{\phi KK} g_{K^* \pi K} \epsilon^\mu(p_\phi) (p_\pi + p_K)_\mu \epsilon^\nu(p_{K^*}) (p_\pi + p_K)_\nu \\
& \times \frac{1}{s - m_K^2 - im_K\Gamma_K(E, T)}
\end{aligned} \tag{A4}$$

where ρ^* is shorthand for $\rho(1450)$, the tildes in \mathcal{M}_{12} are needed in order to tell the two initial ϕ s apart, $q = p_\phi + p_\pi$, $l = p_{\pi'} - p_\omega$, $\tilde{l} = p_{K'} - p_\phi$ and the primed and double-primed variables indicate and distinguish between final states.

REFERENCES

- * electronic address: haglin@theo03.nscl.msu.edu
- [1] C. DeTar, Phys. Rev. D **32**, 276 (1985); C. DeTar and J. Kogut; Phys. Rev. D **36**, 2828 (1987).
 - [2] S. Gottlieb *et al.*, Phys. Rev. Lett. **59**, 347 (1987).
 - [3] M. Dey, V. L. Eletsky, and B. L. Ioffe, Phys. Lett. **B252**, 620 (1990).
 - [4] R. Furnstahl, T. Hatsuda, and Su H. Lee, Phys. Rev. D **42**, 1744 (1990); T. Hatsuda, Y. Koike, and Su. H. Lee, Nucl. Phys. **B394**, 221 (1993); Phys. Rev. D **47**, 1225 (1993).
 - [5] C. Gale and J. Kapusta, Nucl. Phys. **B357**, 65 (1991).
 - [6] C. Song, Phys. Rev. D **48**, 1375 (1993).
 - [7] K. L. Haglin and C. Gale, Nucl. Phys. **B421**, 613 (1994).
 - [8] C. M. Ko and D. Seibert, Phys. Rev. C **49** (1994) 2198.
 - [9] K. Geiger, Phys. Rev. D **46**, 4965 (1992); D **46**, 4986 (1992).
 - [10] K. Geiger and J. Kapusta, Phys. Rev. D **47**, 4905 (1993).
 - [11] K. Geiger, Phys. Rev. D **47**, 133 (1993).
 - [12] E. Shuryak, Phys. Rev. Lett. **68**, 3270 1992.
 - [13] X. N. Wang, Phys. Rev. D **43**, 104 (1991); X. N. Wang and M. Gyulassy, Phys. Rev. D **44**, 3501 (1991).
 - [14] K. Haglin and S. Pratt, Phys. Lett. **B328**, 255 (1994).
 - [15] L. P. Csernai and J. I. Kapusta, Phys. Rev. Lett. **69**, 737 (1992).
 - [16] C. Song, Phys. Rev. D **48**, 1375 (1993); Phys. Rev. D **49**, 1556 (1994).
 - [17] U.-G. Meissner, Phys. Rep. **161**, 213 (1988).
 - [18] G. Jansssen, K. Holinde and J. Speth, Phys. Rev. C **49**, 2763 (1994).
 - [19] Particle Data Group, K. Hikasa *et al.*, Phys. Rev. D **45**, p. II.6–II.11 (1992).
 - [20] J. F. Donoghue and B. R. Holstein, Phys. Rev. D **28**, 340 (1983).
 - [21] E. Byckling and K. Kajantie, *Particle Kinematics*, Wiley & Sons, 23 (1973).
 - [22] K. Haglin, Phys. Rev. C **50**, 1688 (1994).
 - [23] M. Prakash, M. Prakash, R. Venugopalan and G. Welke, Phys. Rep. **227**, 321 (1993); Phys. Rev. Lett. **70**, 1228 (1993).
 - [24] H. A. Weldon, Z. Phys. C **54**, 431 (1992).
 - [25] J. L. Goity and H. Leutwyler, Phys. Lett. **B228** 517 (1989).
 - [26] P. Lichard, Phys. Rev. D **49**, 5812 (1994).
 - [27] Only after computing momentum relaxation and diffusion times can one be relatively certain about this.
 - [28] H. A. Weldon, Phys. Rev. D **28**, 2007 (1983).

FIGURES

FIG. 1. Scattering of the vector V with hadron $\{a\}$ through (a) an s -channel “resonance” R , and (b) through a t -channel in which E indicates the exchanged hadron. Particles $\{a, 1, 2, R, E\}$ are enumerated in the text.

FIG. 2. Scattering rate or width for pions (a) and kaons (b) in an ensemble of pions, kaons and ρ mesons.

FIG. 3. Collision rate of ρ with pions and with kaons.

FIG. 4. Collision rate of ω with pions.

FIG. 5. Collision rate of ϕ with ρ mesons into a $K_1(1270) + K$ final state. Three different widths are used for the exchanged kaon: constant values of 20 and 30 MeV are shown as dashed and dotted curves and an energy-dependent width results in the solid curve.

FIG. 6. Contribution to the overall rate from various channels. The curves correspond to the following reactions. Upper solid is $\phi + \rho \rightarrow K_1(1270) + K$, lower solid is $\phi + \rho \rightarrow a_1(1260) + \rho$, short-dashed is $\phi + \pi \rightarrow K^* + K$, long-dashed is $\phi + \pi \rightarrow b_1(1235) \rightarrow \pi + \omega$, upper-dotted is $\phi + K \rightarrow \phi + K$, lower-dotted is $\phi + K^* \rightarrow \pi + K$, dot-dashed is $\phi + K_1(1270) \rightarrow \rho + K$, double-dot-dashed refers to the reaction $\phi + \rho \rightarrow \pi + \rho$, triple-dot-dashed refers to the reaction $\phi + \pi \rightarrow \rho(1450) \rightarrow \pi + \pi$ and finally, quadruple-dot-dashed refers to $\phi + K \rightarrow \pi + K^*$.

FIG. 7. Total collision rate of ϕ mesons in hot hadronic matter.

FIG. 8. Mean free paths for ρ , ω and ϕ mesons in hot hadronic matter.

TABLES

TABLE I. Coupling constants obtained from the decay widths in Eq. (2.5).

coupling constant	numerical value
$g_{\phi KK}^2/4\pi$	2.71
$g_{\rho\pi\pi}^2/4\pi$	2.94
$g_{K^*\pi K}^2/4\pi$	2.47
$g_{K_1\rho K}^2/4\pi$	0.45 [GeV ⁻¹]
$g_{\phi\rho\pi}^2/4\pi$	0.28 [GeV ⁻¹]
$g_{a_1\rho\pi}^2/4\pi$	0.77 [GeV ⁻¹]
$g_{b_1\omega\pi}^2/4\pi$	0.32 [GeV ⁻¹]
$g_{b_1\phi\pi}^2/4\pi$	7.6×10^{-3} [GeV ⁻¹]
$g_{\rho KK}^2/4\pi$	0.73 ¹
$g_{\rho'\phi\pi}^2/4\pi$	0.20 [GeV ⁻¹]
$g_{\rho'\pi\pi}^2/4\pi$	2.41 ²
$g_{\omega\pi\rho}^2/4\pi$	15.80 ³
$g_{\rho\pi\omega'}^2/4\pi$	6.53 [GeV ⁻¹]

¹This is taken from quark-model arguments to be half of the $\rho\pi\pi$ coupling constant just as in Ref. [8].

²A branching fraction of 90% was assumed.

³This is obtained from vector-meson-dominance arguments to be $g_{\omega\pi\rho} = (e/g_{\rho\pi\pi})^{-1}g_{\omega\pi\gamma}$.

TABLE II. Reactions considered in which the vector meson scatters.

graph number	reaction	intermediate meson	channels	$\bar{\Gamma}(T=200 \text{ MeV})$
ρ meson reactions				
1, 2	$\rho + \pi \rightarrow \rho + \pi$	π	s, t	} 49.5
3, 4	$\rho + \pi \rightarrow \rho + \pi$	ω	s, t	
5, 6	$\rho + \pi \rightarrow \rho + \pi$	ϕ	s, t	
7, 8	$\rho + \pi \rightarrow \rho + \pi$	$a_1(1260)$	s, t	
9, 10	$\rho + \pi \rightarrow \rho + \pi$	$\omega(1390)$	s, t	
11, 12	$\rho + K \rightarrow \rho + K$	$K_1(1270)$	s, t	66.0
ω meson reactions				
1, 2	$\omega + \pi \rightarrow \omega + \pi$	$b_1(1235)$	s, t	} 74.0
3, 4	$\omega + \pi \rightarrow \omega + \pi$	ρ	s, t	
5, 6	$\omega + \pi \rightarrow \pi + \pi$	ρ	s, t	21.2
ϕ meson reactions				
1	$\phi + \rho \rightarrow K_1(1270) + K$	K	t	2.29
2	$\phi + \pi \rightarrow K^*(892) + K$	K	t	6.05
3	$\phi + K^*(892) \rightarrow \pi + K$	K	t	0.78
4	$\phi + K_1(1270) \rightarrow \rho + K$	K	t	0.12
5	$\phi + \rho \rightarrow \pi + \rho$	π	t	0.16
6	$\phi + \rho \rightarrow a_1(1260) + \rho$	π	t	0.07
7,8	$\phi + \pi \rightarrow \pi + \omega$	$b_1(1235)$	s, t	1.57
9,10	$\phi + K \rightarrow \phi + K$	K	s, t	3.89
11	$\phi + \rho \rightarrow K + K$	K	t	0.34
12	$\phi + \phi \rightarrow K + K$	K	t	0.03
13	$\phi + K^*(892) \rightarrow K + \rho$	π	t	0.09
14	$\phi + K \rightarrow K^*(892) + \rho$	π	t	0.85
15	$\phi + K \rightarrow \rho + K$	K	t	3.28
16	$\phi + \pi \rightarrow \pi + \pi$	$\rho(1450)$	s	0.58
17	$\phi + K \rightarrow \pi + K^*$	K	s	7.24

This figure "fig1-1.png" is available in "png" format from:

<http://arxiv.org/ps/nucl-th/9410028v1>

This figure "fig2-1.png" is available in "png" format from:

<http://arxiv.org/ps/nucl-th/9410028v1>

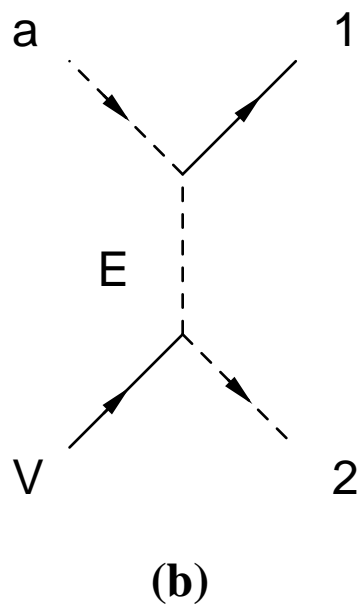
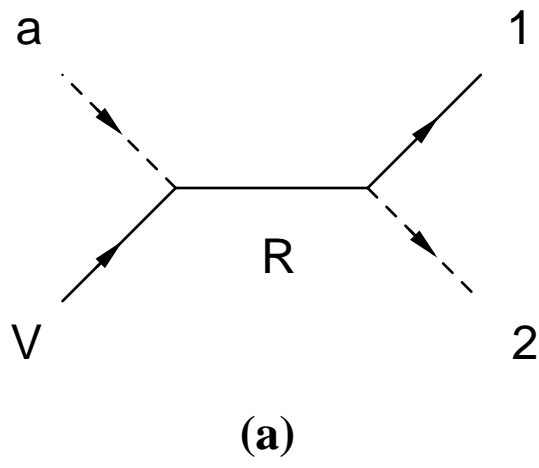


Figure 1

This figure "fig1-2.png" is available in "png" format from:

<http://arxiv.org/ps/nucl-th/9410028v1>

This figure "fig2-2.png" is available in "png" format from:

<http://arxiv.org/ps/nucl-th/9410028v1>

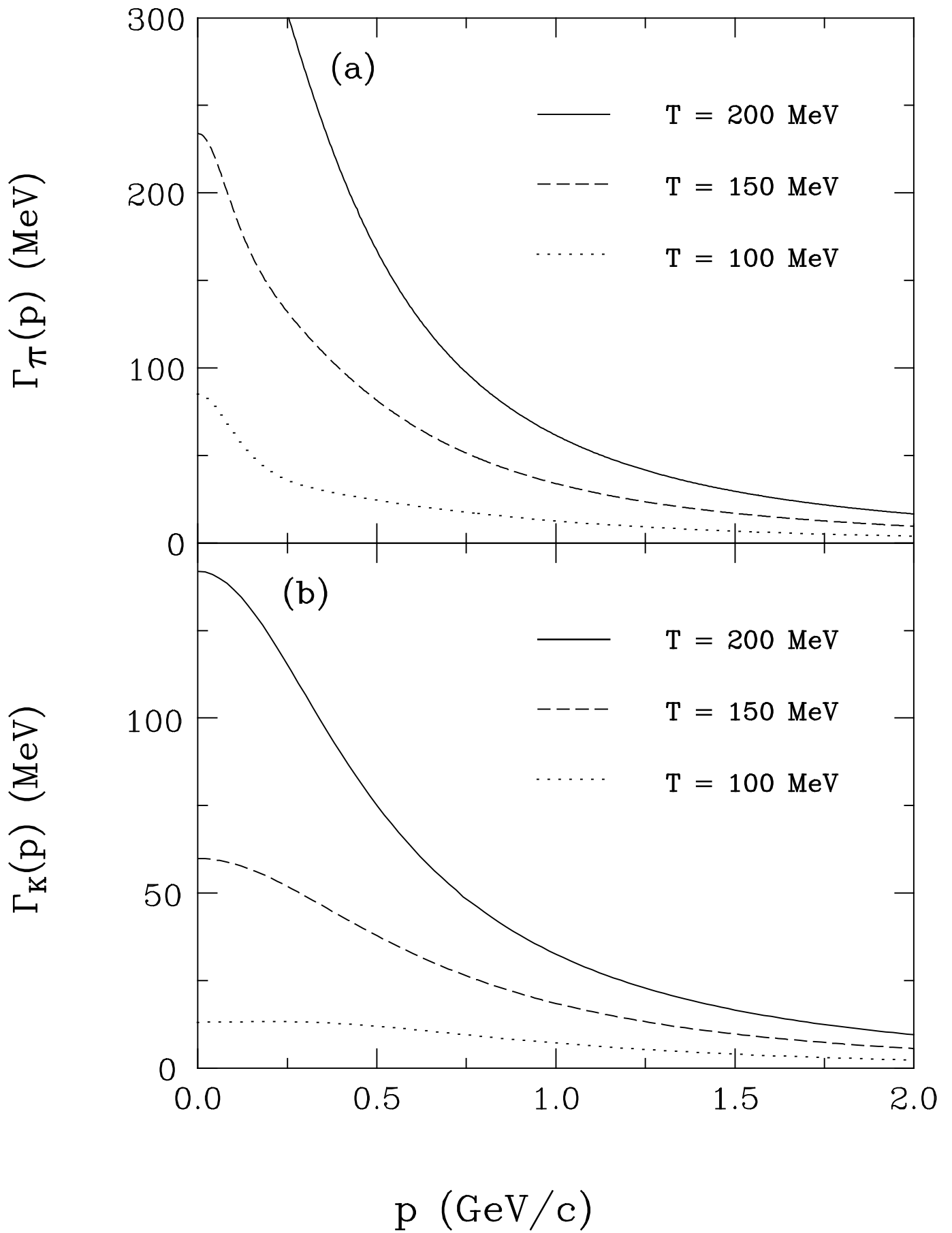


Figure 2

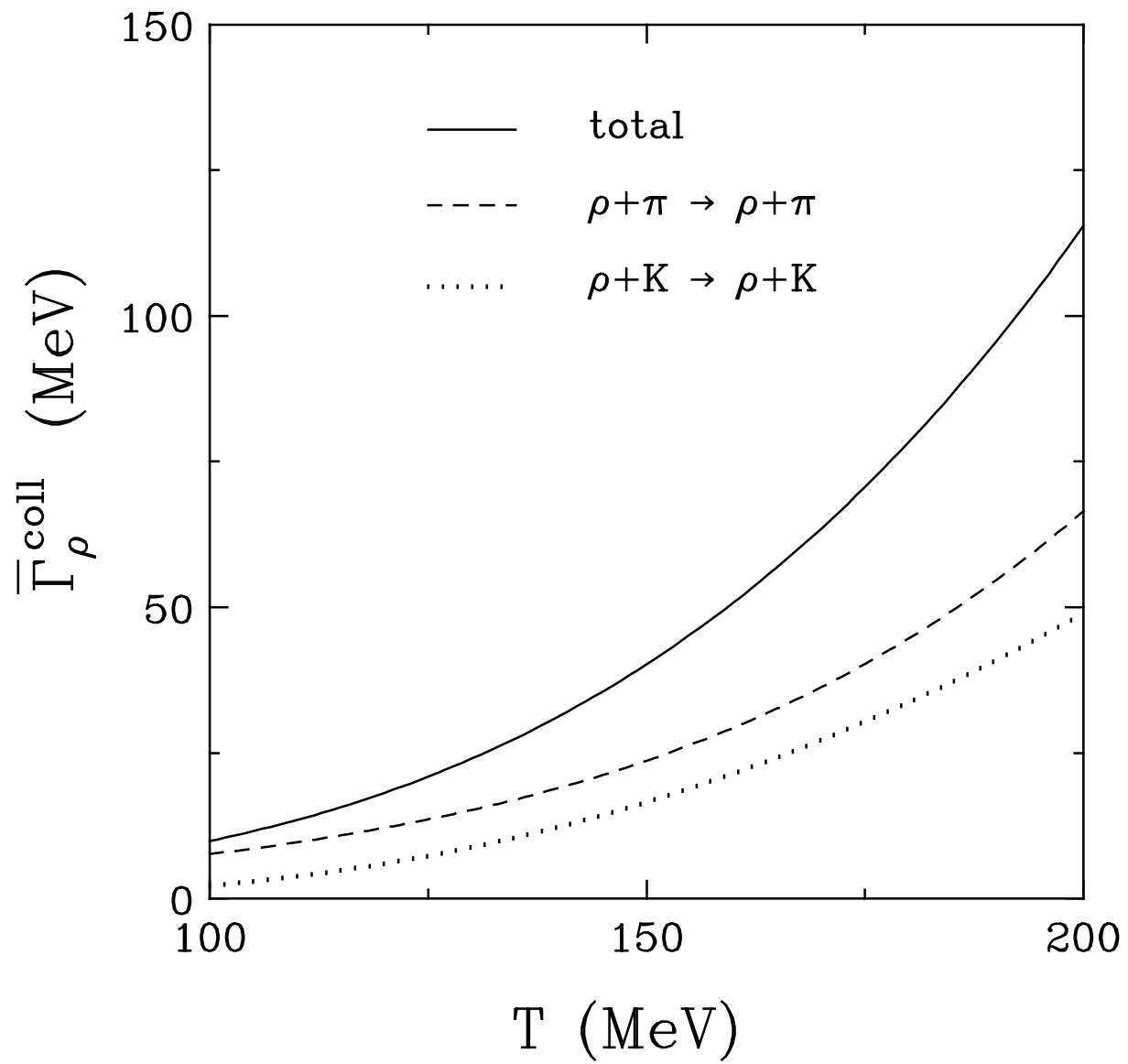
This figure "fig1-3.png" is available in "png" format from:

<http://arxiv.org/ps/nucl-th/9410028v1>

This figure "fig2-3.png" is available in "png" format from:

<http://arxiv.org/ps/nucl-th/9410028v1>

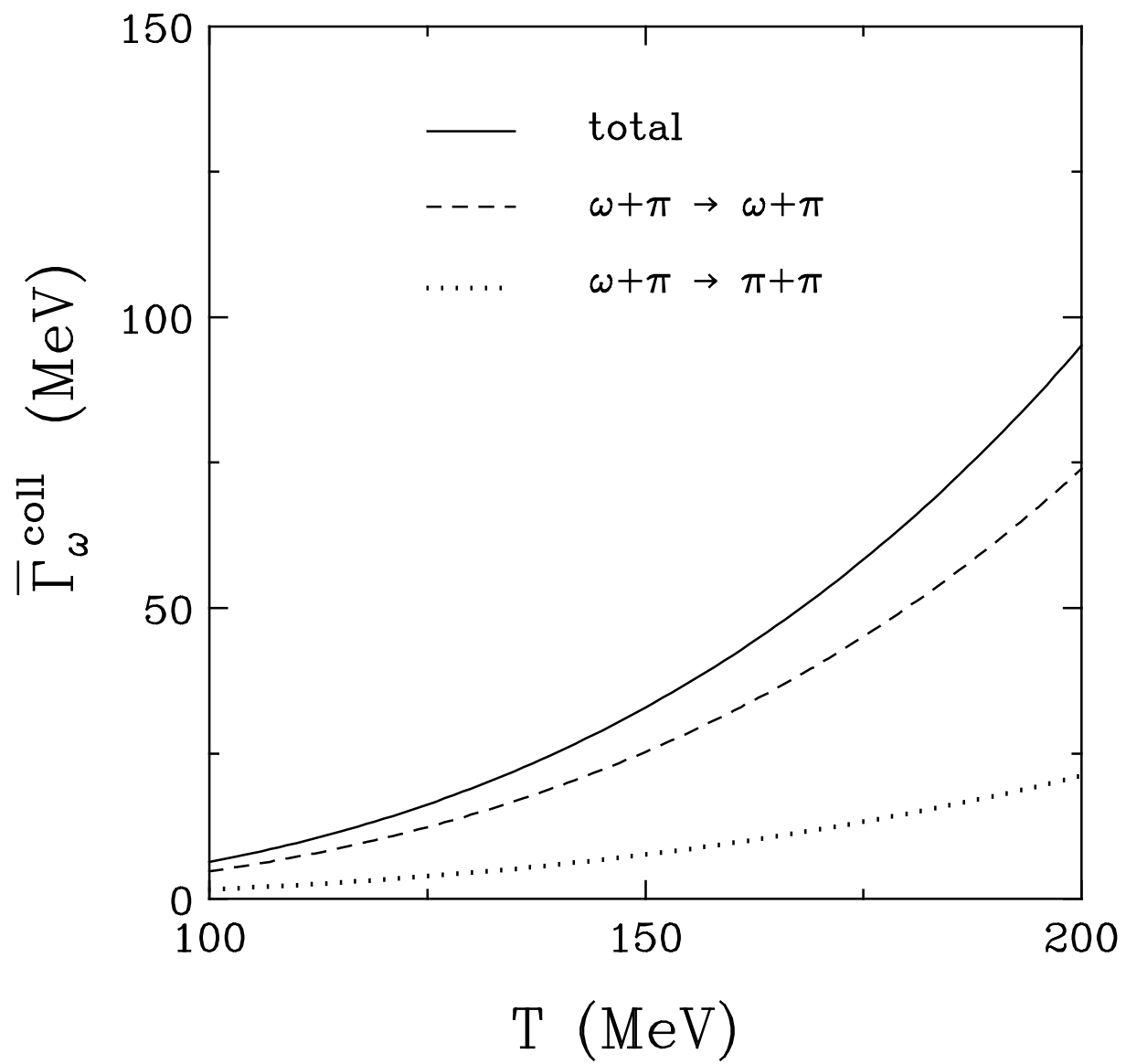
Figure 3



This figure "fig1-4.png" is available in "png" format from:

<http://arxiv.org/ps/nucl-th/9410028v1>

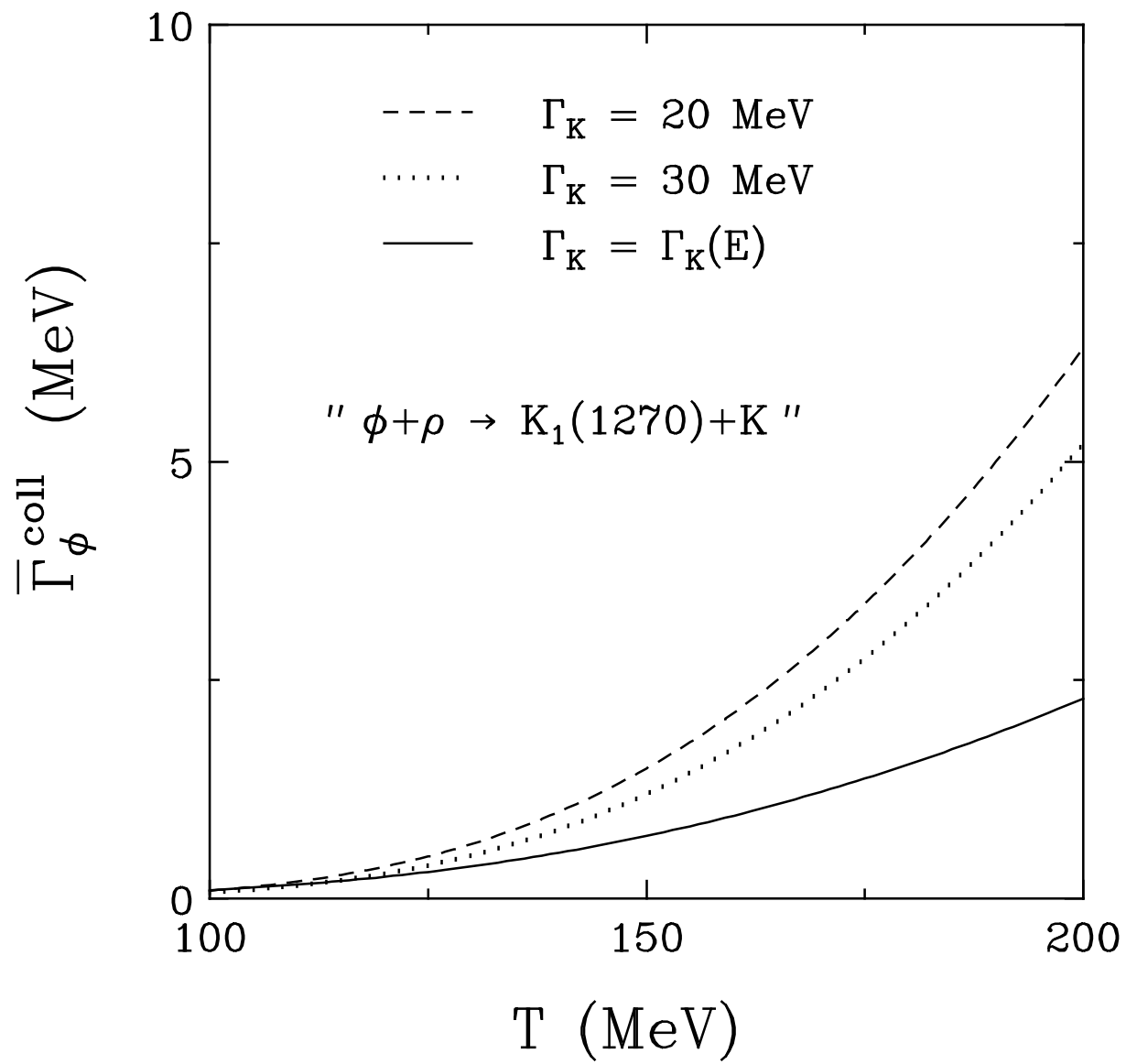
Figure 4



This figure "fig1-5.png" is available in "png" format from:

<http://arxiv.org/ps/nucl-th/9410028v1>

Figure 5



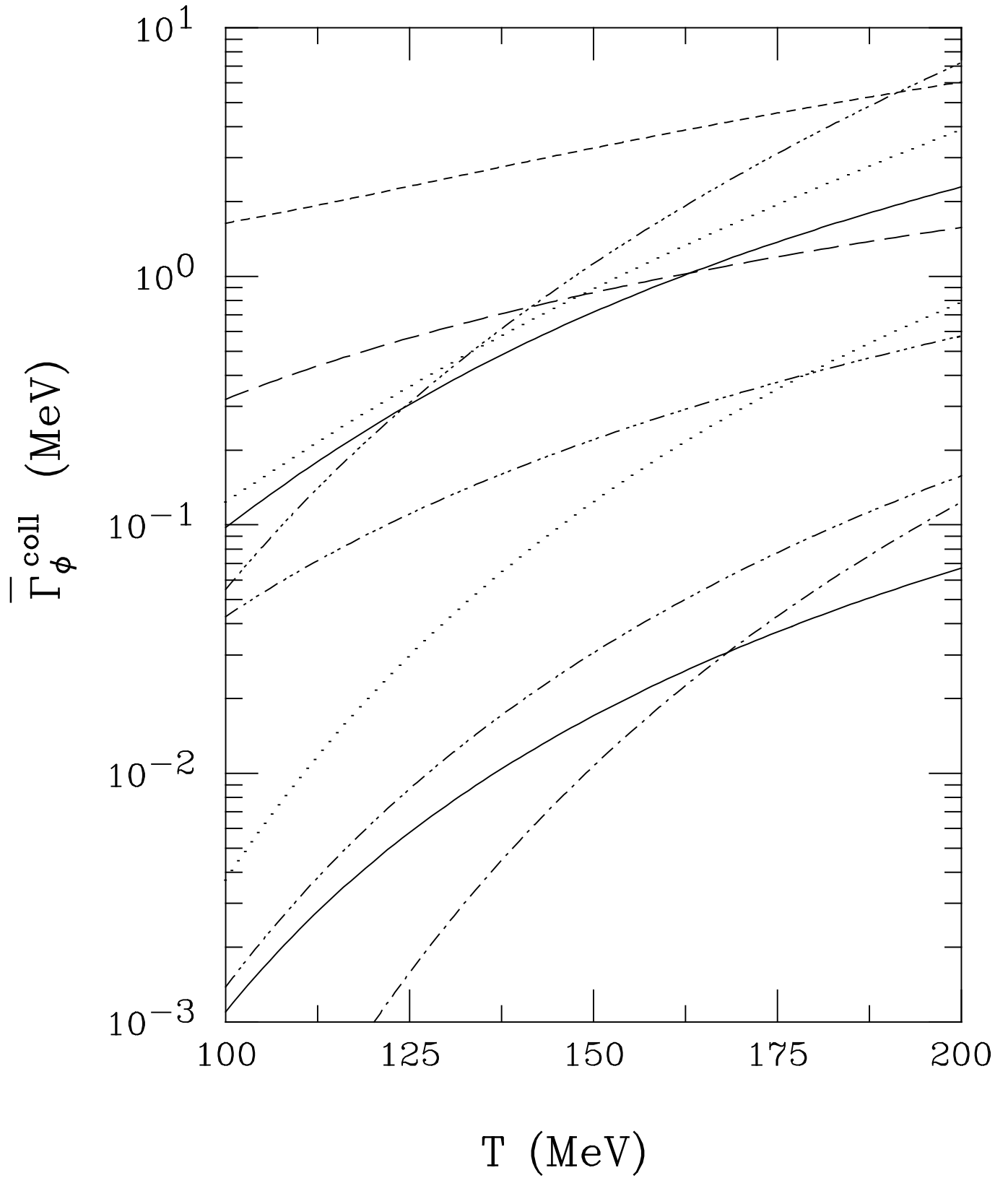


Figure 6

Figure 7

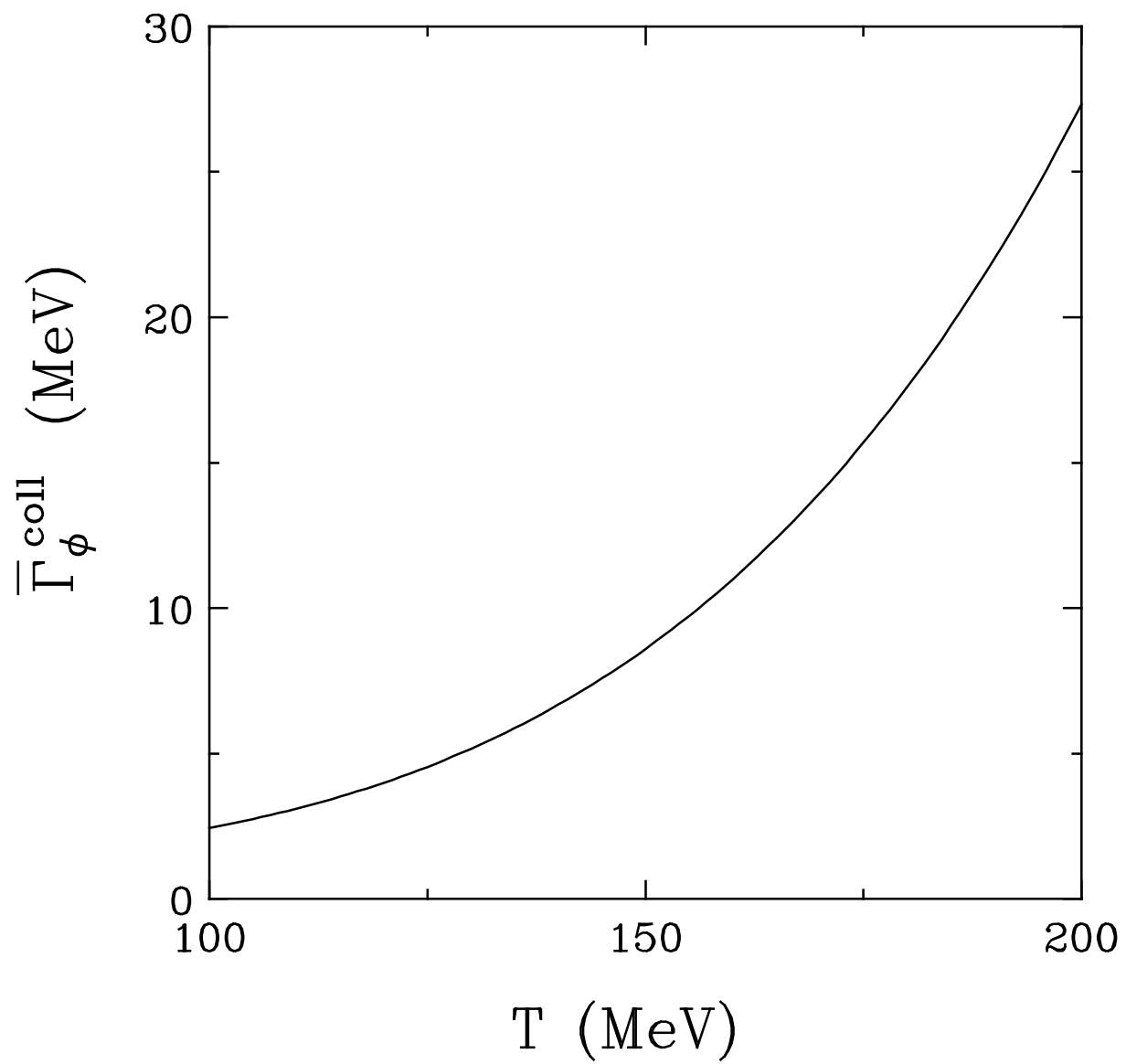


Figure 8

